

Optical Imaging in Biology and Medicine
Master in Photonics & Europhotonics Master Program

Adaptive Optics for Microscopy

Carles Otero Molins

Johannes Rebling

November 19, 2013

Abstract

Lorem ipsum dolor sit amet, qui ei case inani noster, malis tantas expetenda id qui. Vel assum labore intellegat et. Eu vis vero fastidii intellegebat, ea omnis tation definiebas usu. Ea cetero maiorum convenire sed. Wisi impetus aperiri quo at.

Vis tation maiorum facilisis an, quo ei summo pericula consetetur. Illum quodsi euripidis ex est. Duo ea soluta causae sanctus. Eu pro dolorum imperdiet ullamcorper, quas oporteat at pro, ius an appellantur complectitur. Ea nam aperiri fierent invenire, nam in purto illum iracundia, ei facilisi iracundia scribentur ius. Utroque dolores ex est, ius an tation suscipiantur, ne iriure aperiam quaestio mel. Cum enim legere impedit ex, per ut blandit vituperata conclusionemque, ad aliquid vivendum usu.

TODO!

- introduce abbreviations for Adaptive Optics (AO) and Adaptive Optics Microscopy (AOM) in the intro and then use them through the text

Contents

1	Introduction	1
2	Aberration Measurement and Correction	1
2.1	Direct Wavefront Sensing	2
2.2	Indirect Wavefront Sensing	4
2.3	Aberration Correction	5
2.4	Control Strategies	6
3	Adaptive Optics Methods applied in Microscopy	7
3.1	Widefield Microscopy	7
3.1.1	Transmission Microscope	7
3.1.2	Structured Illumination Microscopy	9
3.2	Point Scanning Microscopes	11
3.2.1	Confocal Microscopes	11
3.2.2	Two-Photon Fluorescence Microscopy	12
4	Future Prospects	14
5	Conclusion	15
	References	16

1 Introduction

It is well known that optical aberrations degrade the resolution and brightness of images. That means a reduction in both lateral and axial resolution and a fall in signal intensity. Aberrations, in general terms, can be defined as the wavefront distortions with respect to ideal spheres, these distortions are due to imperfections in any part of the optical system. In microscopy, aberrations may arise from the microscope itself or the specimen under study [7]. Therefore, aberrations always limit in some way the final image quality and vary from one specimen to another, so they cannot be corrected by a fixed optical design. Dynamic correction is necessary.

That is the reason why scientists have been trying to overcome this problem for many years. The best approach to it is what nowadays is called Adaptive Optics (AO). The first proposal of the use of AO technology was suggested in the year 1953 in the context of astronomical optics for the compensation of the aberrating effects of the atmosphere [4].

The main idea of the AO is the modulation of an incoming wavefront in such a way that we can record an image without aberrations. It is based upon the principle of phase conjugation: the correction element introduces an equal but opposite phase aberration to that present in the optical system. In order to do that, we need to be able to measure these distortions reliably. The most direct way is to use a wavefront sensor, the Shack-Hartmann [37, 31] or Curvature Sensors [34] are examples of it. Also, interferometric techniques have been used to measure aberrations [39]. Nevertheless, there are indirect methods in which aberrations are estimated using an algorithm and do not employ a wavefront sensor, they are called sensorless techniques [8]. In addition to the wavefront sensing, we need the adaptive element to modulate the aberrations before the light reaches the imaging detector, this is usually a deformable mirror or a liquid crystal spatial light modulator (LC-SLM). Finally, we need a control system that processes the aberrations information and uses it to monitor the adaptive correction element.

Although Adaptive Optics systems have been introduced in applications such as astronomy, laser beam shaping, optical communications, data storage and ophthalmology [9], when it is applied to microscopy is not always trivial and it requires a different approach than in the other fields. One particularly difficult thing in AO microscopy is how the aberration information is obtained in each of the different microscopy techniques.

The optical microscope techniques can be divided in two main groups: the widefield techniques and the point scanning techniques. Some examples of the first group are the conventional transmission microscopy, the structured illumination microscopy and the fluorescence microscopy. Some examples within the second group are the confocal microscopy or the non-linear microscopy such as Two-Photon Excitation Fluorescence (TPEF), Second Harmonic Generation (SHG), Third Harmonic Generation (THG), Coherent anti-Stokes Raman (CARS) or Stimulated Emission Depletion (STED).

In this report, in order to explain how adaptive optics and microscopy link together, we will start explaining the basis of adaptive optics. That means a brief review of the concept of aberrations and how they are most commonly characterized. After that, we will explain in more detail the main methods for wavefront sensing, the main aberration corrector devices and some control strategies. Finally, we will show some applications of the AO in different widefield and point scanning microscopy techniques. The last part will be a short explanation of future prospects and conclusions.

2 Aberration Measurement and Correction

In practice, no optical system can be totally free from aberrations. That means that all the rays coming from the same object point and going through an optical system will not converge into the same point at the image plane. In other words, the wavefront is distorted with respect to an ideal one when passing through a real system. Thus, we can define the Wavefront Aberration Function as the optical path difference between the aberrated (real) wavefront and the reference (perfect) wavefront. There are some ways to characterize mathematically the aberrations. In systems with circular symmetry (circular apertures) it is very common to use the Zernike polynomials (2.1) because they form a complete, orthogonal set of functions defined over a unit circle. This property gives independence between these

functions. That implies that it is possible to associate to each polynomial a specific an independent weight that will contribute to the description of the Wavefront Aberration Function.

$$W(\rho, \phi) = \sum_n^k \sum_{m=-n}^{m=n} c_n^m Z_n^m(\rho, \phi), \quad (2.1)$$

Where $W(\rho, \phi)$ is the Wavefront Aberration Function in polar coordinates at the exit pupil, c_n^m are the Zernike coefficients and $Z_n^m(\rho, \phi)$ are the Zernike modes (or polynomials). As we can see in the equation, the Wavefront Aberration Function is a linear combination of polynomials. Therefore, the more polynomials (i.e. modes, $Z_n^m(\rho, \phi)$) we get the better characterization of the $W(\rho, \phi)$ function we have. Representing aberrations in this way can simplify the design, control and characterization of the Adaptive Optics system. In general, we can obtain an aberrated wavefront when it is reflected to a non-planar surface or when it is going through an inhomogeneous media (Fig. 1).

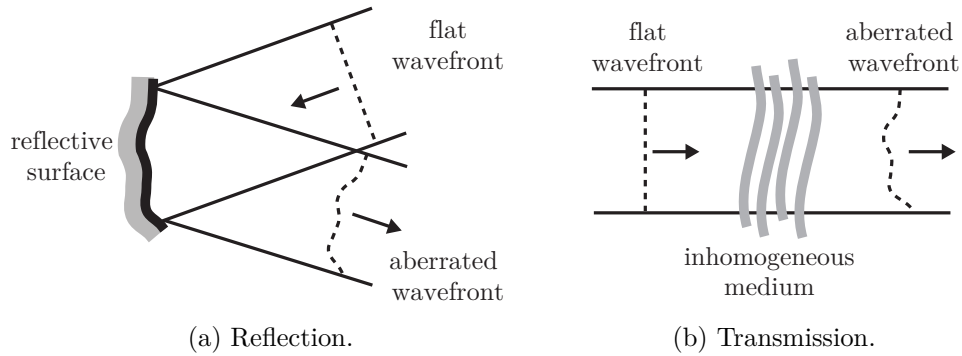


Figure 1: Wavefront aberrations due to (a) reflection from a non planar surface and (b) caused by propagation through a non-uniform refractive index distribution [7].

In biological microscopy, the two potential sources of aberrations are the optics and the specimen under study. Regarding the optics, one important parameter that has to be taken into account is the Numerical Aperture (NA), aberrations become more significant for those microscopes employing higher NA. Regarding the specimen, aberrations comes basically from the variations in refractive index due to the three-dimensional nature of cells and tissue structures. In general, they become greater in magnitude as long as we focus deeper. Also aberrations can be produced by the difference of refractive index between the microscope coverslip and the specimen mounting medium [7]. Although it is known where the aberrations come from, it is not always easy to measure them and implement the measure inside the optical system. There are different classifications of Wavefront Sensing in the bibliography [38]. Here we will use the one of Martin J. Booth [7] and we will explain the most common methods of wavefront sensing applied to microscopy.

2.1 Direct Wavefront Sensing

Direct Wavefront Sensing is based on a direct measure of the phase gradient or the wavefront slope, it is considered as an aperture-plane sensing. Within this group there are several techniques such as interferometric, although in general the most used is the Shack-Hartmann.

This last technique has its origin more than 400 years ago in the Scheiner's Disk developed by the astronomer Christopher Scheiner [37]. Later on, in the twenty century, Hartmann used the Scheiner's Disk to develop a test which measured the wavefront's slope at the exit of the optical system by using a screen with multiple holes. This technique was progressing until the 1971, when Platt and Shack developed a two-dimensional array of a few lenslets -a matrix of microlens-, all with the same diameter and the same focal length, that could substitute the screen with multiple holes. This is the start point of the technique known as "Shack-Hartmann"[31].

This technique allows us to reconstruct the wavefront aberration function from the local slope's

changes of an aberrated wavefront in relation with a reference wavefront. That is achieved measuring the displacements $(\Delta x, \Delta y)$ from each image given by each microlens (Fig. 2).

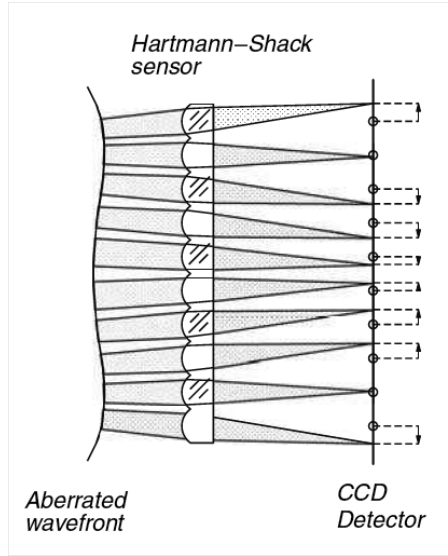


Figure 2: Two-dimensional section of Shack-Hartmann matrix of microlens. When an incoming wavefront goes through the matrix is divided in multiple beams. In the focal plane of the matrix we have multiple spots. If the wavefront is not aberrated each spot will be placed in the axis of each microlens. If it is aberrated, it will be displaced with respect this axis [26].

We start from an aberrated beam going through the matrix of microlens before it is detected in a recorder device. The beam is then spatially sampled into many individual beams (one for each microlens) by the lenslet matrix and forms multiple spots in the focal plane of the lenslets. Finally, the recorder device -that is placed at the focal plane of the matrix- registers multiple spots. This device is usually a CCD camera. The typical lenslet diameters range from about 100 to 600 μm and the typical focal lengths range from a few millimeters to about 30 mm [32].

We must note that direct sensing needs a well defined wavefront in the pupil of the system or in other words, a point-like emitter. An this situation might not happen in biological microscopes where we are studying three-dimensional specimens, because the light emitted by the specimen may come not only from the focal point. This fact brings us to a couple of problematic situations. The first one is the superposition of wavefronts in the pupil which its effects will depend on the coherence of the emitted light. If it is coherent we will have interference in the pupil, thus we will have ambiguous sensor readings and this kind of sensing will not be suitable for aberration correction. In this sense, if in the focal region the specimen behaves as a point-like scatterer (it will emit incoherent light) the sensor will be able to measure the aberrations produced in the emission path, which in principle they should be the same as in the illumination path. But, if our specimen acts as a planar mirror-like in the focal region, the sensor will just be able to measure twice the even components of the aberrations produced in the illumination path (or emission path), that is because the "mirror behaviour" will spatially invert the aberrations in the illumination path (Fig. 3).

Let us analyse it in detail. We denote the illumination $(W(\rho, \phi)_i)$ and emission $(W(\rho, \phi)_e)$ path aberrations as the sum of its even and odd components,

$$W(\rho, \phi)_i = W(\rho, \phi)_i^{\text{even}} + W(\rho, \phi)_i^{\text{odd}}, \quad (2.2)$$

$$W(\rho, \phi)_e = W(\rho, \phi)_e^{\text{even}} + W(\rho, \phi)_e^{\text{odd}}, \quad (2.3)$$

The measured aberration $(W(\rho, \phi))$ is the sum of the illumination and emission path aberrations,

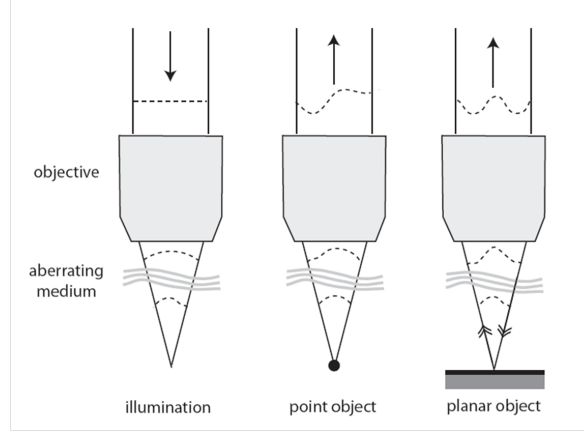


Figure 3: Representation of the two effects due to the specimen structure on wavefront measurements. The left figure shows how the wavefront is aberrated in the illumination path. In the center it is shown a point-like scatterer. Only the emission path is measured. In the right figure it is shown a planar reflector. The illumination wavefront is spatially inverted on reflection before acquiring further aberration in the detection path [7].

$$W(\rho, \phi) = W(\rho, \phi)_i^{even} + W(\rho, \phi)_i^{odd} + W(\rho, \phi)_e^{even} + W(\rho, \phi)_e^{odd}, \quad (2.4)$$

Due to the spatial inversion we know that,

$$W(\rho, \phi)_i^{even} = W(\rho, \phi)_e^{even} \quad (2.5)$$

$$W(\rho, \phi)_e^{odd} = -W(\rho, \phi)_i^{odd} \quad (2.6)$$

Then, the aberration measured can be simplified,

$$W(\rho, \phi) = 2W(\rho, \phi)_e \quad (2.7)$$

We have shown that in planar mirror-like structures we lose information about aberrations. Thus, in this cases it is not a good option to implement a direct sensing. Regarding microscopy techniques, we must note here that fluorescence emission is an incoherent process, but the non-linear processes generate a coherent signal.

The other problematic situation that we can have in direct sensing due to three-dimensional nature of the specimen is that our sensor might detect more intensity signal from the light scattered out-of-focus than the scattered in the focal region. In order to overcome this problem it can be used a spatial filter between objective and sensor. This filter performs in a similar way than the pinhole used in confocal microscopy. Also it is possible to use coherence gating to exclude out-of-focus light instead of the spatial filter, although it is a more complex method. We must recall here that the light emitted in the non-linear processes is confined mostly in the focal region.

2.2 Indirect Wavefront Sensing

While direct wavefront sensing techniques are widely applied in Astronomy, they are less common in microscopy techniques. This for several reasons. It is not as easy to create a guiding star like point source in a biological specimen. If there are not features in the specimen that occur there naturally

and which resemble a point source, one has to be implemented manually which might alter the function of the specimen or might even be toxic to the sample. Modern microscopes are also highly complex and optimized, which makes it difficult to insert a relatively large wavefront sensor. For samples with weak signal strength, it is also desirable to collect as many photons as possible for the imaging process. Splitting the beam and using a part of the light emitted from the sample for direct wavefront sensing might hence decrease the signal strength too much.

Indirect techniques do not measure the wavefront directly but instead optimize the image quality. This leads to the retrieval of the aberration and the necessary corrections. Hence these techniques don't sense the wavefront but rather improve the image quality and through this correct for wavefront aberrations. Indirect methods are used more often in industrial and medical applications. They usually require very little additional hardware. Once the technique is optimized for a specific problem, indirect schemes are easier to implement in practice and are more prone to errors due to the lack of additional hardware (a single deformable mirror might be sufficient to implement adaptive optics in an existing microscope).

Indirect techniques include phase diversity as well as optimization of an image quality metric. Phase diversity techniques use two or more images of an extended object to make an estimation of the distorting wavefront [16]. However, this technique still requires a beam splitter, a second detector and a deformable mirror which is a significant disadvantage over image quality metric optimization where only the normally recorded image and a deformable mirror is required. It is also necessary to record images with different focus positions and hence the each phase retrieval step takes many seconds. Therefore the entire process of optimizing the wavefront takes minutes, which is too slow for most biological imaging [23]. It is for these reasons that phase diversity techniques are less common in microscopy and will not be described further. The focus of this section is therefore a general description of image quality metric techniques. Their specific properties and how they are implemented in the different microscopy techniques is then described in Section 3.

The optimization of an image quality metric is mainly a mathematical rather than a technical problem. We will describe the basic principle but the derivation of the specific metrics is beyond the scope of this paper. The interested reader will find more information on the mathematical background in reference [33, 6, 24, 13].

For these techniques, the aberration correction is performed through an iterative optimization of an image quality metric based. The metric is usually based on spatial frequencies [13] or image intensity [18]. Such optimization is either implemented empirically or by using an appropriate mathematical model. In many practical systems aberrations can be accurately represented by a small number of modes of an orthogonal basis, such as Zernike polynomials. A sequence of images is acquired, each with a different aberration applied and the correction aberration is estimated from the information in these images. This process is repeated until the image quality is considered acceptable. The number of measurements needed to obtain an acceptable image depends strongly upon the optimization algorithm and parameters used, the mathematical representation of the aberration, and the object structure. For the earliest and most generic algorithms the number of measurements per aberration mode increases quadratically or exponentially with N , the number of corrected aberration modes [6]. The so called direct maximization method (as described in Section 3.1.1) is significantly more efficient, requiring only $N + 1$ measurements for N modes. With this technique, Lukosz polynomials [24] are used to classify the aberrations. The effects of different modes can then be separated and the optimization of each mode becomes independent and hence more efficient.

An effective model-based adaptive optics scheme should also be independent of the imaged object and should permit the separation of aberration and object influences on the measurements. This separation is also possible through the appropriate choice of optimization metric and aberration representation [13].

2.3 Aberration Correction

The wavefront correctors are the essential device of an adaptive optics system. Their aim is to provide a certain phase profile of the incident wavefront by changing the physical length over which the wavefront propagates or the refractive index of the medium through which the wavefront passes. They

are based on mirror technology (Fig. 4) or on liquid crystal technology. The first ones change the phase by adjusting their surface shape (i.e., change their physical length while keeping the refractive index constant) and the second ones keep the physical length constant and rely on localized changes in refractive index. The mirror-based correctors are wavelength and polarisation independent and can be reconfigured at rates of a few kilohertz [7]. They can have a continuous surface (i.e., discrete actuator, bimorph or membrane mirrors) or segmented surface (i.e. piston-only or piston/tilt mirrors). Unlike continuous mirrors, the segmented mirrors have gaps between the segments that reduce the efficiency and quality of the correction, although they can achieve much better wavefront fitting.

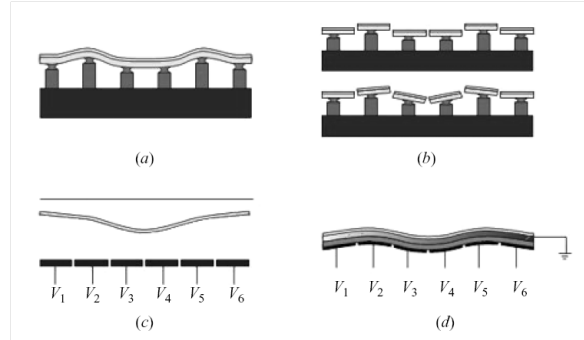


Figure 4: The four main mirror correctors [32]. (a) Discrete actuator deformable mirrors consist of a continuous, reflective surface and an array of actuators, each capable of producing a local deformation in the surface. (b) Piston-only segmented correctors consist of an array of small planar mirrors whose axial motion (piston) is independently controlled. Piston/tip/tilt-segmented correctors add independent tip and tilt motion to the piston-only correctors. (c) Membrane mirrors and (d) Bimorph mirrors.

Regarding the liquid crystal-based mirrors, they change the refractive index electronically or optically, are wavelength and polarisation dependent and can reach velocities of just a few tens of hertz. The nematic liquid crystal is the most common for AO applications. In general, they are much cheaper than the mirror-based correctors, are capable of producing more complex phase patterns but they have lower light efficiency.

In AO microscopes the first choice in most cases is the deformable mirror because of their high detection efficiency. Besides, they are better suited for fluorescence techniques due to their polarisation independent behaviour. However, in particular cases, LC-SLM can be enough if aberration correction is only needed in the illumination path.

2.4 Control Strategies

3 Adaptive Optics Methods applied in Microscopy

Adaptive optics techniques have found their way into almost all kinds of modern, high resolution microscopy techniques. These microscopes have been combined with direct wavefront sensing and sensorless AO, using deformable mirrors or spatial light modulators for aberration compensation (all of which has been described in Section 2. This includes standard widefield microscopes as well as highly sophisticated and specialized point scanning methods such as Coherent Antistokes Raman Spectroscopy (CARS) and STimulated Emission Depletion (STED) techniques. It has to be noted however, that some of these methods are themselves only a few years old. Therefore, they are still being optimized and so are the AOM techniques. It is therefore an interesting field of research with new ideas being implemented every year.

AO was first used in confocal and two-photon fluorescence microscopy, both of which are commonly used in biomedical applications. These microscopes suffer from a significant drop in signal and resolution as the focus is moved deeper into the specimen, which is caused by aberrations.[36]

AOM is also used for imaging of live specimens. Due to an increased excitation signal and improved light collection from the specimen, acquisition times can be reduced and contrast can be enhanced. Techniques that without AO are too slow for live imaging might now be usable, opening up completely new fields of research. Another advantage of AO lies in the microscopy design. Using AO methods, can help the designer to relax the aberration tolerance. This permits a significant reduction in the complexity of the optical system while maintaining diffraction limited operation.

This section will describe, using state of the art examples, how AO is implemented in both widefield and point scanning systems.

3.1 Widefield Microscopy

As mentioned above, AO techniques are being applied in widefield microscopy. In conventional microscopes, widefield illumination is provided using back light illumination or in the case of reflection or fluorescence modes, via the objective lens. The image quality depends only on the aberrations induced in the detection path and is independent of the aberrations of the illumination path. Aberration correction is therefore only necessary in the detection path and a single pass adaptive optics system will suffice [25]. Hence, the goal of AO for widefield microscopy is to restore the best possible imaging and to correct for aberrations induced both by an imperfect imaging system as well as by the imaged specimen. The latter becomes more important for thick biological samples where the light has to travel a larger distance through a medium with an inhomogeneous refractive index.

Many other highly specialized widefield microscopy techniques have been developed and for most of those, AO schemes for aberration correction and resolution optimization have been presented. Two widefield microscopy techniques will be presented in this section. First the implementation of AO in a standard transmission microscope (Section 3.1.1) using a sensorless wavefront sensing scheme is explained. How the theoretical background of this technique can be applied to more sophisticated microscopy schemes is then shown on the example of structured light illumination (Section 3.1.2), a specialized wide field technique.

Not covered by this report is the application of AO using a direct wavefront sensing scheme as presented by *Azucena et al.* in 2011 using a Shack–Hartmann wavefront sensor, a fluorescent reference source, and a deformable mirror[3]. Adaptive optics can also be used to correct for aberrations in fluorescence microscopy. There, the aberration caused by a refractive index mismatch between sample, cover plate and immersion medium can be calculated theoretically and is then corrected [22] or the aberration is measured using a guide-star technique [2] as described in section 2. AO is also applicable in multifocal multiphoton microscopy [5, 12].

3.1.1 Transmission Microscope

To implement adaptive optics with standard (incoherent) transmission microscopes, *Debarre et al.* [13] implement an indirect, sensorless and image-based adaptive optics scheme, as shown in Fig. 5. As described earlier in Section 2.2, image-based techniques do not require an additional wavefront sensor

but retrieve the correction data directly from the recorded images. As with all indirect sensing schemes, the difficulty is to find a good metric for image quality, which allows to determine the appropriate correction parameters.

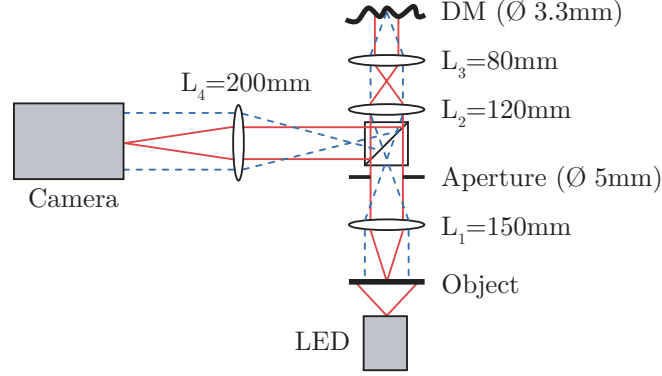


Figure 5: Schematic diagram of the experimental setup, showing a simple microscope complemented with a deformable mirror for aberration correction. Image after [13].

The presented method uses low spatial frequency content of the image as the optimization metric. The aberration is represented in terms of so called Lukosz modes. Like Zernike polynomials, the Lukosz functions are each expressed as the product of a radial polynomial and an azimuthal function. The presented technique is based on modeling the effects of aberrations on the imaging of low spatial frequencies, which Lukosz modes are found to be ideal for.

By modeling the aberration $\Phi(r)$ as a series of N Lukosz modes $L_i(r, \phi)$ with coefficients a_i [24]:

$$\Phi(r) = \sum_{i=4}^{N+3} a_i L_i(r, \phi), \quad (3.1)$$

they develop the optimization metric g as the sum of a range of low frequencies. It is related to the coefficients of the aberration expansion, a_i by the Lorentzian function [13]

$$g(a_i) \approx \frac{1}{q_0 + q_1 \sum_{i=4}^{N+3} a_i^2} \quad (3.2)$$

where the piston, tip and tilt modes ($i = 1, 2, 3$ respectively) have been omitted and q_0 and q_1 are both positive quantities in the frequency range of interest. The aberration correction process is then performed as the maximization of $g(a_i)$. Because of this particular aberration expansion and optimization metric, the function $g(a_i)$ shows a paraboloidal maximum that permits the use of simple maximization algorithms. Furthermore, it is shown that the optimization can be performed as a sequence of independent maximizations for each aberration coefficient.

The correction process is shown in Figure 6 for the correction of a single Lukosz mode using a scatterer specimen. Using the deformable mirror (DM), an initial aberration a_i is applied and an image is recorded. The Fourier transform and spectral density of the image are then calculated and the appropriate range of frequency components are summed, giving the metric measurements g_0 . The same procedure is repeated with both negative and positive aberrations (i.e. stronger and weaker aberrations), resulting in the metric measurements g_- and g_+ . Due to the parabolic maximum of (3.2), the value of a_i that minimizes g can be calculated from as little as three measurements of $g(a_i)$. The optimum correction aberration can then be estimated by parabolic minimization as [33]:

$$a_{\text{corr}} = \frac{b(g_+ - g_-)}{2g_+ - 4g_0 + 2g_-} \quad (3.3)$$

and is then applied to the DM. To correct multiple modes, each modal coefficient is measured in the same manner before the full correction aberration containing all modes is applied. While this technique

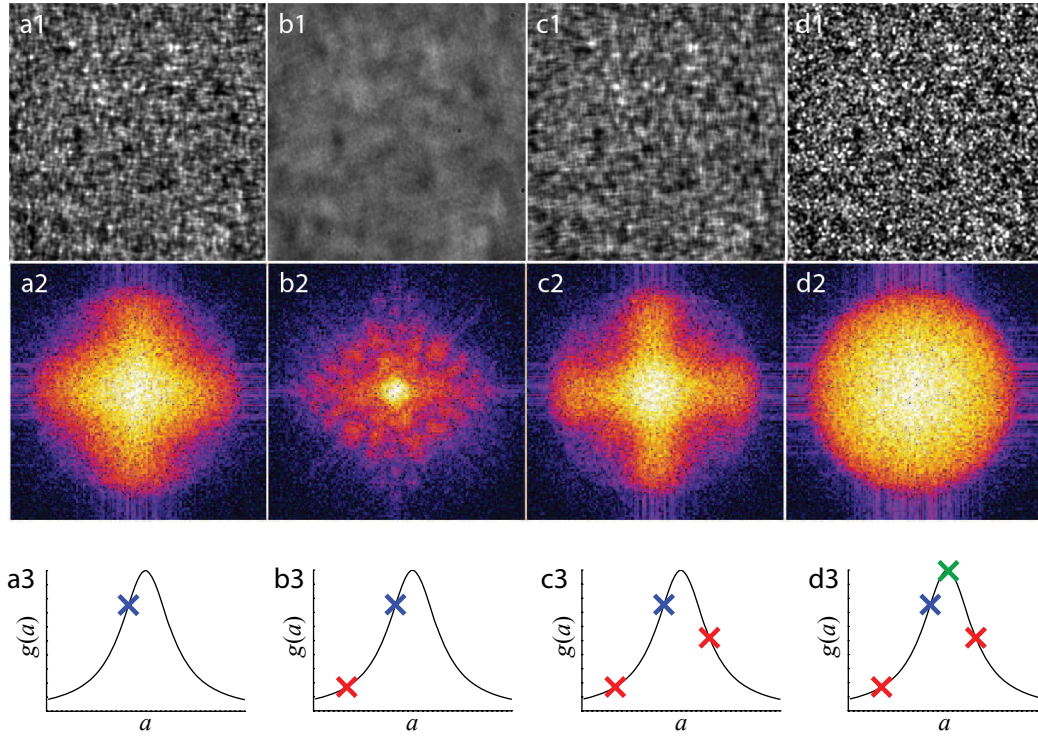


Figure 6: Correction of a single Lukosz aberration mode (astigmatism, $i = 5$) for a scatterer specimen and using low spatial frequencies. The first row shows the raw images of the specimen and the second row contains the corresponding spectral densities. The third row illustrates schematically the sampling of the Lorentzian curve used in the optimization calculation. (a1-a3) correspond to an arbitrary initial aberration of magnitude, (b1-b3) have an additional negative bias while (c1-c3) have an additional positive bias of equal magnitude. (d1-d3) show the corrected image calculated with the parabolic minimization. Image after [13].

is based only on low spatial frequencies, it is shown that both low and high frequency components can be effectively corrected. In all the cases investigated, a Strehl ratio greater than 0.8, close to the diffraction limit, was obtained. This indicates that, when aberration statistics are unknown, choosing small spatial frequencies for an initial correction is a reasonable strategy. If further correction is required, they can be performed using a larger range of frequencies. *Debarre et al.* conclude that this correction scheme is largely independent of the object structure and propose that this approach also to be valid for coherent or partially coherent systems.

3.1.2 Structured Illumination Microscopy

It is often desired for biological samples to produce clear images of focal planes deep within a thick sample (i.e. optical sectioning) and common techniques include point-scanning techniques such as confocal or multiphoton techniques which are described in Section 3.2.

Widefield techniques such as Structured Illumination (SI) microscopy can also provide optical sectioning. However, there the sectioning is realized using a standard microscopes, an incoherent light source and without the need for a scanning mechanism. For SI microscopy, a grid is imaged into the specimen to produce a one-dimensional sinusoidal excitation pattern in the focal plane. The resulting sinusoidal fluorescence image, consisting of both in-focus and out-of-focus fluorescence emission, is then normally recorded. Several images are taken, each corresponding to a different grid position equivalent to three different phase shifts of the grating. The grid pattern only appears in the focal plane while it is blurred in the out of focus regions. Hence, it is possible to extract an optical section from the spatially modulated component of the images via a simple calculation.

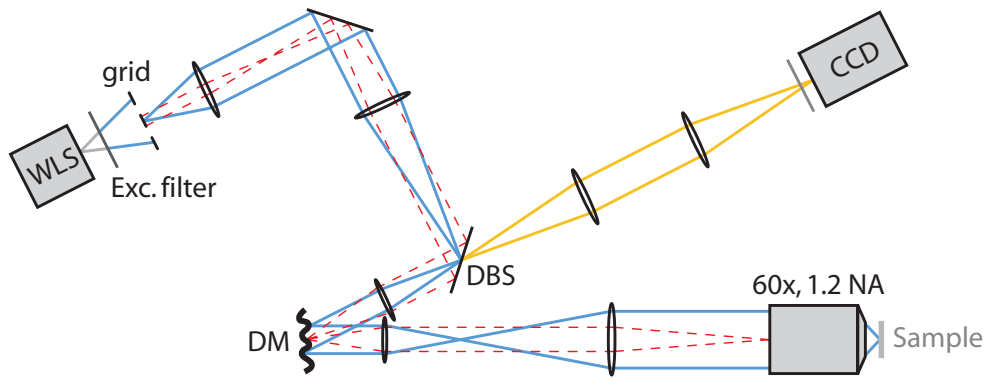


Figure 7: Experimental setup for structured illumination microscopy with aberration correction. WLS - white light source, DM - deformable mirror, DBS - dichroic beamsplitter. The blue rays mark the illumination path; the detection path is shown in yellow. Image after [14] .

Based on the SI microscopy technique presented by *Neil et al.* in 2005 [28] as well as their earlier work on indirect wavefront sensing using a conventional microscope [13] in 2007 (described in the previous section) *Debarre et al.* combined both techniques in 2008 and proposed an AO scheme for use in SI microscopy [14].

They again present a sensorless wavefront detection scheme, which is shown in Fig. 7. The method to obtain the aberration correction is similar to the one presented and explained in the previous section. The authors derive an inner product from a mathematical model of the imaging process, followed by an orthogonalization process applied to a set of Zernike polynomials. Based on that, a general method providing an optimal aberration expansion for the chosen optimization metric is presented. This process yields information about the effects of different aberration modes in of the SI microscope. *Debarre et al.* show that the image quality mainly depends on the imaging efficiency spatial frequency of the illumination pattern. This imaging efficiency is affected much more by some aberration modes (called grid modes) than by others (called non-grid modes) . Grid modes have a significant influence on the intensity of the sectioned image, whereas non-grid modes have comparatively little effect. The non-grid modes do however affect the resolution.

The results of the implemented AO scheme is shown in Fig. 8 for aberration correction on a fluorescent mouse intestine. The image contrast and sharpness improvement is clearly visible in image 8b compared to the uncorrected image in 8a. As a result of the aberration correction, and as shown in Fig. 8c, the contrast of small sample features (blue arrows) is better defined after (red solid line) rather than before (black dotted line) correction.

The authors also explain an additional benefit of aberration correction for structured illumination microscopy. That the adaptive element can also be used to improve the rejection of the out-of-focus fluorescence. When imaging thick specimen, noise fluctuations in the fluorescence signal between the three successive widefield images obtained for the maximization process result in a large out-of-focus background in the calculated sectioned images. Since this background arises from fluorescence generated outside the focal plane, it is not sensitive to the presence of aberrations. By applying large aberrations in a number of grid modes, the grid pattern is suppressed and only the out-of-focus noise can be measured. By subtracting this aberrated image from the original sectioned image, the fluorescent background can be efficiently removed, leading to greatly improved contrast of the in-focus structures.

The aberrations can also change significantly with depth and hence using the same correction for different depths can result in a degradation of the image quality. The correction can however be adapted for different imaging depths in the sample. This permits improvement of the image quality throughout an axially extended sample. It is furthermore possible to determined the appropriate modes once and use the same scheme for any specimen, as the scheme is mostly independent of the object structure. Alternatively, if one wants to correct for local variations in aberrations the image could be formed from several sub-images for which independent aberration correction would be performed.

In conclusion, the authors present a sophisticated, easy to implement and highly versatile AOM

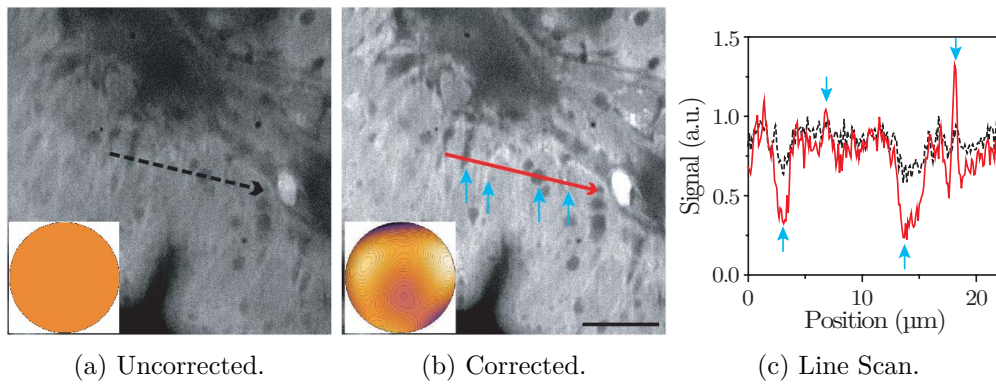


Figure 8: Aberration correction in structured illumination microscopy. A fluorescent mouse intestine sample was imaged (a) without (b) with aberration correction with inserts showing the phase induced by the deformable mirror. (c) Profile along the lines drawn on the images, both profiles normalized so that their mean value is identical. As a result of the resolution improvement, the contrast of small sample features (blue arrows) is better defined after (red solid line) rather than before (black dotted line) correction. The imaging depth was approximately $10\text{ }\mu\text{m}$, scale bar size $10\text{ }\mu\text{m}$. Image after [14] .

scheme which allows for aberration correction induced by the optical system, the specimen or the focus depth. While the presented scheme uses a widefield microscope, *Debarre et al.* are also optimistic that similar AO methods based on indirect, image based aberration detection can be applied to point-scanning methods.

3.2 Point Scanning Microscopes

Just as with the widefield techniques, adaptive optics quickly found its way into point scanning techniques to improve the image and signal quality.

Scanning methods are useful for imaging biological specimens, since they can provide high resolution imaging in three-dimensions. Illumination is usually provided by a laser that is focused into the sample. The light emitted or reflected from the specimen is collected, usually through the same objective lens, and its intensity is measured by a detector. Since this only provides information about the intensity at a single spot, focal point is then scanned through the specimen and point-by-point the image is acquired.

Several other point scanning microscope modalities have been introduced, including Two-Photon Excitation Fluorescence (TPEF) microscopy, second harmonic generation (SHG) and third harmonic generation (THG) microscopy, and coherent anti-Stokes Raman (CARS) microscopy.

- using a fluorescence microscope, the smaller FWHM, provided by the optimized DMM, will increase the excitation intensity leading to a higher fluorescent signal for the same laser beam input power

3D adaptive optics in a light sheet microscope [11] [21] -> Both the second- and third-harmonic intensity signals are used as the optimization metric. Aberration correction is performed to compensate both system- and specimen-induced aberrations by using an efficient optimization routine based upon Zernike polynomial modes. Images of live mouse embryos show an improved signal level and resolution.

[29] -> THG, based on indirect wavefront sensing using total image intensity as metric

[40] ->

[19]

-

3.2.1 Confocal Microscopes

The confocal microscopy can be operated in reflection or fluorescence mode. Both are a dual pass system, which means that either the illumination path and the emission path have to be corrected in an AO confocal microscope.

The first attempt to apply AO in confocal microscopy was done by *Martin J. Booth et al* [?]. They implement indirect wavefront sensing to a confocal fluorescence microscope in a closed-loop way. Aberration measurement and correction was done sequentially. First a preset positive bias aberration was introduced by the mirror. An image scan was taken and all of its pixel values were summed and averaged to give the value of W_1 . Then, it was added to the system the equivalent negative bias aberration, obtaining W_2 . They had shown before that the value of the difference signal, $W = W_1 - W_2$, is approximately proportional to the amount of the Zernike mode Z_i present. They applied this procedure for several different Zernike modes, updating the mirror shape each time. The experimental set-up is shown in

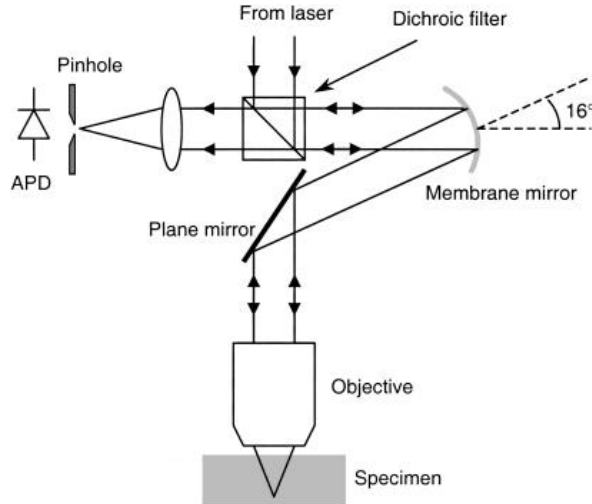


Figure 9: A beam from a frequency-doubled Nd:YAG laser (wavelength 532 nm) was passed through a beam expander. The illumination beam was reflected by the membrane mirror such that the angle between the incident and reflected beams was 16° . The illumination beam then passed via a plane mirror and relay lenses (not shown) into the objective lens focusing the light into the specimen. Fluorescence light from the specimen was collected by the same objective and followed a reciprocal path, through the membrane mirror, and then was transmitted through the filter block. The light was focused through a pinhole onto an avalanche photodiode (APD). In this configuration, the membrane mirror can compensate for aberrations introduced into both the illumination and emission optical paths.

This dual pass adaptive system can usually be implemented using a single deformable mirror, if the path length aberrations are the same for both the illumination and the emission light. This is the case if there is no significant dispersion in the specimen or chromatic aberration in the optics.

A pinhole is not required to obtain three-dimensional resolution, so most TPEF microscopes use large area detectors to maximise signal collection. Although they rely upon other physical processes, non-linear imaging modalities such as SHG, THG and CARS exhibit similar resolution properties. When using large area detectors, the fidelity of imaging in the detection path is unimportant so the effects of any aberrations in this path are negated. It follows that single pass adaptive optics is appropriate for these microscopes as aberration correction need only be implemented in the illumination path.

[30] [10]

3.2.2 Two-Photon Fluorescence Microscopy

Its intrinsic optical sectioning, larger penetration depth, reduced photo damage as well as other advantages allowed nonlinear microscopy in general, and Two-Photon Fluorescence Microscopy (TPFM) in particular, to become a very important tool in biological imaging since its first presentation by *Denk et al.* in 1990 [17].

As with most AO microscopy techniques, both a direct and indirect wavefront sensing scheme can be deployed for the use with TPFM. Indirect sensing was already explained (section 2.2) and pre-

sented (section 3.1 in detail. *Marsh et al.* present the first and fairly simple indirect sensing approach, correcting only for depth induced aberrations as early as 2003 [27]. Again, based on their earlier works ([13, 14]), *Débarre et al.* present another highly sophisticated application of their image based wavefront sensing scheme in 2009 [15]. Both *Marsh* and *Débarre* essentially use the standard TPFM setup and the image optimization is very similar to the one presented earlier, we will not describe these methods here again.

Rueckel et al. present a wavefront correction method using coherence-gated wavefront sensing [35] which also beyond the scope of this report. This section will therefore describe direct wavefront sensing based on the work presented by *Aviles-Espinosa et al.* in 2011 [1].

The resolution has a high dependence on the point-spread function (psf) of the scanned point source. Additionally, the signal levels in two-photon fluorescence have a strong nonlinear dependence upon the incident light intensity. Thus the ideal is to image the sample by use of a diffraction limited spot. However, refractive-index mismatches between the immersion media of high-NA objectives and the sample, in addition to the usually nonuniform samples themselves, impart aberrations to the wavefront and contribute to a deterioration of the psf. Other sources of aberrations include off-axis transmission through optical components, such as the objective and scan lenses while scanning, and imperfections in the optical elements throughout the optical train. The net effect of specimen induced aberrations is that while reducing the achievable resolution, the necessary laser power to achieve imaging increases with depth which can lead to nonreversible effects in biological samples. It also places greater demands in terms of output power on multiphoton imaging laser sources.

- no need to correct on the collected beam as light is only emitted in focus region - correcting the excitation beam is a must as this will ensure a better focusing and therefore, a more efficient nonlinear (NL) process - sensor-less schemes, iterative algorithms are generally used to control a deformable mirror (DM) or a Spatial Light Modulator - it has been reported the use of optimized algorithms reduce sample exposure - still implies that an area of interest within the sample has to be exposed a considerable number of times - may result in unwanted exposure which is prone to produce photo-bleaching and photo-toxic effects on the sample - We demonstrate that sample induced aberrations can be measured and corrected, - In sensor-based schemes correction performed by measuring aberrations through a wavefront sensor - employing a reference point source called guide star - Then such information is fed to a DM, in order to restore the image quality. - information is then fed into an adaptive element and aberration is corrected - all explained in detail in 2.1 - guide star has been applied for moderate scattering samples imaged through linear fluorescence microscopy [2] - artificially inserting a small, fixed secondary light source inside the sample - allows for a direct measurement of the sample aberrations using a Shack-Hartmann (SH) WFS, - based on the introduction of beads inside the sample - it is prone to cause sample damage, limiting its potential for in vivo imaging studies - beads are randomly distributed inside the fixed sample, suitable bead placed at the right location must be found in the field of view (FOV) and for each depth to be imaged - adds complexity to the sample preparation and to the aberration measurement process - Two-photon excited fluorescence (TPEF) naturally produces a small confined volume which can be used as an incoherent secondary light source - this point source, authors refer to as "nonlinear guide-star" (NL-GS), can be used for single pass measurements of sample and objective aberrations - uses the fact that two-photon excited fluorescence naturally produces a localized point source inside the sample: the nonlinear guide-star (NL-GS). - The wavefront emitted from the NL-GS can then be recorded using a Shack-Hartmann sensor. - Compensation of the recorded sample aberrations is performed by the deformable mirror in a single-step. - applied to fixed and in vivo biological samples, showing, in some cases, more than one order of magnitude improvement in the total collected signal intensity. - measured using a WFS placed at the output port of the NLM microscope - as the WF is directly expressed in the form of Zernike coefficients, it is possible to shape the adaptive element (DM) in a single step (i.e. without the need of any search algorithm) for correcting the measured aberrations - so, image quality and contrast can be significantly improved without having to expose the sample for large periods of time - Consequently photo-bleaching and photo-toxicity are greatly reduced - it can be applied in vivo, it is simple, noninvasive and requires no additional sample processing (such as the incorporation of fluorescent beads) - Moreover, the NL-GS can be created at any desired position inside a sample - has been demonstrated with both, moderate and increased scattering samples. - For

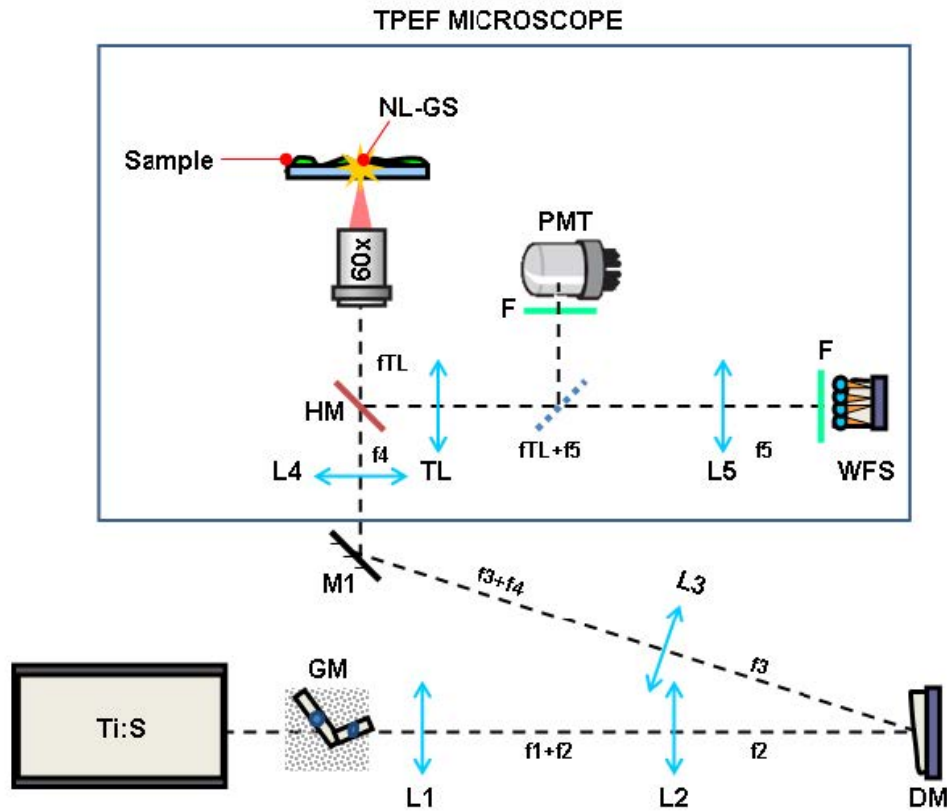


Figure 10: check if we really want this...[1] Use it...do it yourself and make it nice!!!

moderate scattering samples, when comparing coupling vs. focusing aberrations, we found that the total signal improvement can be up to 11.66 times - For samples with increased scattering correction is moderate but in agreement with other adaptive optics correction schemes

[1]

4 Future Prospects

More work must be done before AO can become a regular component of laboratory microscopes. Most AO microscopes are too complex to set up, and their application can be limited by the robustness of operation. The development of automated alignment and calibration procedures would enable the turnkey operation needed to make these systems more practical.

The effectiveness of AO microscopy is mostly compromised by aberration measurement, rather than by currently available correction devices. More sophisticated wavefront sensors or sensorless optimization schemes will extend the microscope's ability to cope with large and more complex aberrations. An obvious goal is to develop "realtime" aberration sensing to increase the speed of correction. Coupled to this is the desire to reduce the exposure of specimens during the measurement process—an essential step when using microscopes for live imaging.

Aberrations can change significantly across a single field of view because the refractive index of the specimen varies throughout its volume. So far, the methods used in adaptive microscopes have provided only a fixed aberration correction for each image. This is sufficient if the imaged region is small enough that aberrations do not vary significantly across the field.

One way to overcome this limitation would be to apply multiconjugate AO to microscopes. This method has been applied in astronomy using multiple deformable mirrors to compensate for multiple aberrating layers in the atmosphere. A similar approach in microscopy would compensate for the 3-D refractive index distribution, although the optical system would become considerably more complex.

Further advances in AO will extend the capabilities of high-resolution microscopes to reveal functional and structural information from deep within biological tissue. Currently, optimum performance is often

limited to thin regions near to the coverslip, sufficient for imaging individual cells, but of rather limited practicality for tissue imaging. AO promises to help move microscopy into a new regime in which biological studies that were previously confined to cell cultures can be performed in thick tissue and even in live specimens.

Add short part about STORM/PALM which are not using adaptive optics yet... [20],

5 Conclusion

abberations that are important for imaging system differ a lot, some need correction of both illu and imaging, some use direct, other indirect methods, some only need correction of some abberation modes, others need as much as possible...important to choose correct system for given problem and figure it our in detail before ordering something

AO is applicable to almost all microscopy techniques...

Is image based aberration detection and correction as performed in [13] and [14] done in point scan techniques?

References

- [1] Rodrigo Aviles-Espinosa, Jordi Andilla, Rafael Porcar-Guezenec, Omar E. Olarte, Marta Nieto, Xavier Levecq, David Artigas, and Pablo Loza-Alvarez. Measurement and correction of in vivo sample aberrations employing a nonlinear guide-star in two-photon excited fluorescence microscopy. *Biomed. Opt. Express*, 2(11):3135–3149, Nov 2011.
- [2] Oscar Azucena, Justin Crest, Jian Cao, William Sullivan, Peter Kner, Donald Gavel, Daren Dillon, Scot Olivier, and Joel Kubby. Wavefront aberration measurements and corrections through thick tissue using fluorescent microsphere reference beacons. *Opt. Express*, 18(16):17521–17532, Aug 2010.
- [3] Oscar Azucena, Justin Crest, Shaila Kotadia, William Sullivan, Xiaodong Tao, Marc Reinig, Donald Gavel, Scot Olivier, and Joel Kubby. Adaptive optics wide-field microscopy using direct wavefront sensing. *Opt. Lett.*, 36(6):825–827, Mar 2011.
- [4] H. W. Babcock. The possibility of compensating astronomical seeing. *Pub. Astron. Soc. Pacific*, 65:229+, Oct 1953.
- [5] Jörg Bewersdorf, Rainer Pick, and Stefan W. Hell. Multifocal multiphoton microscopy. *Opt. Lett.*, 23(9):655–657, 5 1998.
- [6] Martin Booth. Wave front sensor-less adaptive optics: a model-based approach using sphere packings. *Opt. Express*, 14(4):1339–1352, Feb 2006.
- [7] Martin J Booth. Adaptive optics in microscopy. *Philosophical Transactions of the Royal Society A: Mathematical, Physical and Engineering Sciences*, 365(1861):2829–2843, 2007.
- [8] Martin J. Booth. Wavefront sensorless adaptive optics for large aberrations. *Opt. Lett.*, 32(1):5–7, Jan 2007.
- [9] Martin J. Booth, Delphine Débarre, and Alexander Jesacher. Adaptive optics for biomedical microscopy. *Opt. Photon. News*, 23(1):22–29, 1 2012.
- [10] Martin J. Booth, Mark A. A. Neil, Rimas Juškaitis, and Tony Wilson. Adaptive aberration correction in a confocal microscope. *Proceedings of the National Academy of Sciences*, 99(9):5788–5792, 4 2002.
- [11] Cyril Bourgenot, Christopher D. Saunter, Jonathan M. Taylor, John M. Girkin, and Gordon D. Love. 3d adaptive optics in a light sheet microscope. *Opt. Express*, 20(12):13252–13261, Jun 2012.
- [12] Simao Coelho, Simon Poland, Nikola Krstajic, David Li, James Monypenny, Richard Walker, David Tyndall, Tony Ng, Robert Henderson, and Simon Ameer-Beg. Multifocal multiphoton microscopy with adaptive optical correction. *Proc. SPIE*, 8588:858817–858817–12, 2013.
- [13] Delphine Debarre, Martin J. Booth, and Tony Wilson. Image based adaptive optics through optimisation of low spatial frequencies. *Opt. Express*, 15(13):8176–8190, 6 2007.
- [14] Delphine Débarre, Edward J. Botcherby, Martin J. Booth, and Tony Wilson. Adaptive optics for structured illumination microscopy. *Opt. Express*, 16(13):9290–9305, 6 2008.
- [15] Delphine Débarre, Edward J. Botcherby, Tomoko Watanabe, Shankar Srinivas, Martin J. Booth, and Tony Wilson. Image-based adaptive optics for two-photon microscopy. *Opt. Lett.*, 34(16):2495–2497, 8 2009.
- [16] Ross W. Deming. Phase retrieval from intensity-only data by relative entropy minimization. *J. Opt. Soc. Am. A*, 24(11):3666–3679, Nov 2007.

- [17] W Denk, JH Strickler, and WW Webb. Two-photon laser scanning fluorescence microscopy. *Science*, 248(4951):73–76, 1990.
- [18] J. R. Fienup and J. J. Miller. Aberration correction by maximizing generalized sharpness metrics. *J. Opt. Soc. Am. A*, 20(4):609–620, Apr 2003.
- [19] Travis J. Gould, Daniel Burke, Joerg Bewersdorf, and Martin J. Booth. Adaptive optics enables 3d sted microscopy in aberrating specimens. *Opt. Express*, 20(19):20998–21009, 9 2012.
- [20] Audrius Jasaitis, Grégory Clouvel, and Xavier Levecq. Extreme precision in 3d: Adaptive optics boosts super-resolution microscopy. Visited on 12/11/13.
- [21] Alexander Jesacher, Anisha Thayil, Kate Grieve, Delphine Débarre, Tomoko Watanabe, Tony Wilson, Shankar Srinivas, and Martin Booth. Adaptive harmonic generation microscopy of mammalian embryos. *Opt. Lett.*, 34(20):3154–3156, 10 2009.
- [22] P. KNER, J.W. SEDAT, D.A. AGARD, and Z. KAM. High-resolution wide-field microscopy with adaptive optics for spherical aberration correction and motionless focusing. *Journal of Microscopy*, 237(2):136–147, 2010.
- [23] Peter Kner, Lukman Winoto, David A. Agard, and John W. Sedat. Closed loop adaptive optics for microscopy without a wavefront sensor. *Proc. SPIE*, 7570:757006–757006–9, 2010.
- [24] W. Lukosz. Der einfluß der aberrationen auf die optische Übertragungsfunktion bei kleinen orts-frequenzen. *Optica Acta: International Journal of Optics*, 10(1):1–19, 1963.
- [25] Virendra N. Mahajan. *Optical Imaging and Aberrations, Part II. Wave Diffraction Optics (SPIE Press Monograph Vol. PM209)*. SPIE Press, 2 edition, 8 2011.
- [26] Daniel Malacara, editor. *Optical Shop Testing (Wiley Series in Pure and Applied Optics)*. Wiley-Interscience, 3 edition, 7 2007.
- [27] P. Marsh, D. Burns, and J. Girkin. Practical implementation of adaptive optics in multiphoton microscopy. *Opt. Express*, 11(10):1123–1130, 5 2003.
- [28] M. A. A. Neil, R. Juskaitis, and T. Wilson. Method of obtaining optical sectioning by using structured light in a conventional microscope. *Opt. Lett.*, 22(24):1905–1907, Dec 1997.
- [29] Nicolas Olivier, Delphine Débarre, and Emmanuel Beaufepaire. Dynamic aberration correction for multiharmonic microscopy. *Opt. Lett.*, 34(20):3145–3147, 10 2009.
- [30] James Pawley, editor. *Handbook of Biological Confocal Microscopy*. Springer, 3rd edition, 8 2006.
- [31] B. C. Platt and R. Shack. History and principles of shack-hartmann wavefront sensing. *Journal of refractive surgery*, 17(5), October 2001.
- [32] Jason Porter, Hope Queener, Julianna Lin, Karen Thorn, and Abdul A. S. Awwal. *Adaptive Optics for Vision Science: Principles, Practices, Design and Applications (Wiley Series in Microwave and Optical Engineering)*. Wiley-Interscience, 1 edition, 7 2006.
- [33] William H. Press, Saul A. Teukolsky, William T. Vetterling, and Brian P. Flannery. *Numerical Recipes 3rd Edition: The Art of Scientific Computing*. Cambridge University Press, 3 edition, 9 2007.
- [34] François Roddier. Curvature sensing and compensation: a new concept in adaptive optics. *Appl. Opt.*, 27(7):1223–1225, Apr 1988.
- [35] Markus Rueckel, Julia A. Mack-Bucher, and Winfried Denk. Adaptive wavefront correction in two-photon microscopy using coherence-gated wavefront sensing. *Proceedings of the National Academy of Sciences*, 103(46):17137–17142, 2006.

- [36] M. Schwertner, M. Booth, and T. Wilson. Characterizing specimen induced aberrations for high na adaptive optical microscopy. *Opt. Express*, 12(26):6540–6552, 12 2004.
- [37] Larry N. Thibos. Principles of hartmann-shack aberrometry. In *Vision Science and its Applications*. Optical Society of America, 2000.
- [38] Robert Tyson. *Adaptive Optics Engineering Handbook (Optical Science and Engineering)*. CRC Press, 1 edition, 11 1999.
- [39] Ingolf Weingaertner and Michael Schulz. Interferometric methods for the measurement of wavefront aberrations. *Proc. SPIE*, 1781:266–279, 1993.
- [40] A. J. Wright, S. P. Poland, J. M. Girkin, C. W. Freudiger, C. L. Evans, and X. S. Xie. Adaptive optics for enhanced signal in cars microscopy. *Opt. Express*, 15(26):18209–18219, 12 2007.